Stability Analysis and Geometric Calibration of Off-the-Shelf Digital Cameras

Ayman Habib and Michel Morgan

Abstract

Recent developments of digital cameras in terms of the size of a Charged Coupled Device (CCD) and Complementary Metal Oxide Semiconductor (CMOS) arrays, as well as reduced costs, are leading to their applications in traditional and new photogrammetric, surveying, and mapping functions. Such cameras require careful calibration to determine their metric characteristics, as defined by the Interior Orientation Parameters (IOP), which are essential for any photogrammetric activity. Moreover, the stability of the estimated IOP of these cameras over short and long time periods has to be analyzed and quantified. This paper outlines the incorporation of straight lines in a bundle adjustment procedure for calibrating off-the-shelf/low-cost digital cameras. A framework for automatic extraction of the straight lines in the images is also presented and tested. In addition, the research introduces new approaches for testing the camera stability, where the degree of similarity between reconstructed bundles using two sets of IOP is quantitatively evaluated. Experimental results with real data proved the feasibility of the line-based self-calibration approach. Analysis of the estimated IOP from various calibration sessions over long time periods revealed the stability of the implemented camera.

Introduction

The main objective of photogrammetry is generating high quality, three-dimensional information from two-dimensional imagery. The accuracy of the derived positional information from imagery depends on the validity of the available Interior Orientation Parameters (IOP) of the implemented camera. Determining the IOP requires some control information, which is usually available in the form of a calibration test field. Acquired imagery over the calibration test field is incorporated in a bundle adjustment with self-calibration procedure to estimate the IOP of the camera under consideration. In traditional camera calibration activities, control information takes the form of distinct and specifically marked points/targets (Fryer, 1996). These targets are established and precisely measured in a test field using surveying techniques. The number and distribution of the targets are vital for the recovery of the IOP of the implemented camera. Establishing and maintaining a conventional calibration test field, as well as carrying out the calibration procedure, requires professional surveyors and photogrammetrists. Such requirement limits the potential use of recently available, high quality, and low cost digital cameras in industrial, medical, archeological, security, and transportation applications. Therefore, more efficient calibration techniques, which could be carried out by amateur users of digital cameras, are overdue.

The manipulation of linear features, especially straight lines, is a promising alternative for camera calibration. Using straight lines is advantageous for several reasons. First, they can be easily established in a calibration test field. On the other hand, corresponding image space linear features can be precisely extracted using image-processing techniques. For camera calibration purposes, object space straight lines are valuable since they will project into the image space as straight lines in the absence of distortion. Therefore, deviations from straightness in the image space can be modeled and attributed to various distortion parameters (e.g., radial and de-centering lens distortions) in a near continuous way along the line. Brown (1971) introduced the plumb-line method, which is based on straight lines, to derive an estimate of the radial and de-centering lens distortions. The plumb-line method removes deviations from straightness in image space straight lines using radial and de-centering lens distortion models whose parameters are estimated through an adjustment procedure. This is a rapid and practical approach for computing lens distortion parameters. However, the results would be contaminated by uncorrected systematic errors. Moreover, a separate calibration procedure for determining the principal distance and other systematic distortions, such as affine deformations, is still needed. Guoqing *et al.* (1998) and Prescott and McLean (1997) used straight lines in a multi-stage calibration strategy (i.e., the IOP are sequentially estimated). Heuvel (1999) proposed another approach using straight lines to recover the IOP of the camera. This method can only be applied when dealing with imagery containing parallel and perpendicular lines. Similar to the plumb-line methods, the above approaches start by estimating radial and de-centering lens distortion. Then, the principal point coordinates and the focal length are determined later. Bräuer-Burchardt and Voss (2001) developed a methodology for detecting image space circles while considering them as distorted straight lines. These circles are used later for estimating the distortion parameters. However, lens distortions do not necessarily result in a circular effect of one radius of curvature along the line. Chen and Tsai (1990) introduced another method for incorporating straight lines instead of points for camera calibration purposes. However, this approach requires the knowledge of the parametric equations of the object space straight lines, which mandates additional fieldwork. Habib *et al.* (2002a; 2002b) proposed a calibration test field consisting of straight lines and tie points. Acquired imagery over the test field is used in a bundle adjustment with self-calibration procedure

Department of Geomatics Engineering, University of Calgary, 2500 University Drive NW, Calgary, AB, T2N 1N4, Canada (Habib@geomatics.ucalgary.ca; Mfmorgan@ucalgary.ca).

Photogrammetric Engineering & Remote Sensing
Vol. 71, No. 6, June 2005, pp. 733–741.

0099-1112/05/7106–0733/$3.00/0

to simultaneously estimate the IOP of the implemented camera and the Exterior Orientation Parameters (EOP) of the exposure stations.

Regardless of the calibration procedure, estimated IOP from different calibration sessions have to be inspected to check the stability of the implemented camera. Statistical testing can be utilized to accept or reject the hypothesis that the estimated IOP from these calibration sessions are equivalent. However, this methodology does not provide a meaningful measure of the equivalency of the IOP in terms of useful photogrammetric quantities (e.g., discrepancies in the object space arising from using different IOP). In this research, the stability analysis will be quantitatively evaluated by investigating the degree of similarity between the reconstructed bundles from two sets of IOP.

The following section briefly discusses expected distortion models in imagery captured by digital cameras. Afterwards, the utilization of object space straight lines in a bundle adjustment with self-calibration procedure, according to the methodology proposed by Habib *et al.* (2002-a, 2002-b), is outlined. A strategy for automatic extraction of linear features from calibration imagery is also explained in the same section. Then, the new approach for assessing camera stability is presented. Finally, experimental results, conclusions, and recommendations for future research are summarized.

Self-Calibration: Distortion Models

During camera calibration, one is interested in determining the IOP of the involved camera(s), which comprise the coordinates of the principal point, the principal distance, and image coordinate corrections that compensate for various deviations from the collinearity model. There are four principal sources of departure from collinearity, which are "physical" in nature (Fraser, 1997). These are the radial lens distortion, de-centering lens distortion, image plane un-flatness, and in-plane image distortion. The net image displacement at any point from its theoretical location is the cumulative influence of these perturbations. The relative magnitude of each one of these perturbations depends very much on the quality of the camera being employed.

Radial lens distortion is usually modeled by polynomial series, Equation 1 (Kraus, 1997). The term K_1 alone will usually suffice in medium accuracy applications involving low cost digital cameras. The inclusion of K_2 and K_3 terms might be required for high accuracy applications involving wide-angle lenses:

$$\begin{aligned} \Delta x_{RLD} &= K_1 (r^2 - 1)x + K_2 (r^4 - 1)x + K_3 (r^6 - 1)x \\ \Delta y_{RLD} &= K_1 (r^2 - 1)y + K_2 (r^4 - 1)y + K_3 (r^6 - 1)y \end{aligned} \quad (1)$$

where:

$$r = \sqrt{(x - x_p)^2 + (y - y_p)^2},$$

K_1, K_2, and K_3 are the radial lens distortion parameters, and x_p and y_p are the image coordinates of the principal point.

A lack of centering of the lens elements along the optical axis gives rise to the second category of lens distortion, namely, de-centering distortion. The misalignment of the lens components causes both radial and tangential distortions, which can be modeled by correction equations as follows (Brown, 1966):

$$\begin{aligned} \Delta x_{DLD} &= P_1 (r^2 + 2x^2) + 2P_2 xy \\ \Delta y_{DLD} &= P_2 (r^2 + 2y^2) + 2P_1 xy \end{aligned} \quad (2)$$

where P_1 and P_2 are the de-centering lens distortion parameters.

Systematic image coordinate errors due to focal plane un-flatness can limit the accuracy of photogrammetric triangulation. To compensate for focal plane un-flatness, the focal plane needs to be topographically measured. Then, a third or fourth-order polynomial can model the resulting image coordinate perturbations. Radial image displacement induced by focal plane un-flatness depends on the incidence angle of the imaging ray. Narrow angle lenses of long focal length are not significantly influenced by out-of-plane image deformation, which is usually the case for small format digital cameras.

In-plane distortions are usually manifested in differential scaling between x and y image coordinates. In addition, in-plane distortions might introduce non-orthogonality between image axes. These distortions are usually denoted "affine deformations" and can be mathematically modeled according to Equation 3. One should note that affine deformation parameters, which are correlated with other camera interior and exterior orientation parameters, are eliminated from Equation 3. For example, shifts are eliminated since they are correlated with the principal point coordinates:

$$\begin{aligned} \Delta x_{AD} &= -A_1 x + A_2 y \\ \Delta y_{AD} &= A_1 y \end{aligned} \quad (3)$$

where A_1 and A_2 are the affine distortion parameters (A_1 corresponds to half of the scale difference along the x and y axes while A_2 represents the non-orthogonality angle).

In traditional camera calibration, converging imagery is acquired over a test field with numerous control points, which are precisely surveyed prior to the calibration process. Image and object coordinate measurements are used in a bundle adjustment with self-calibration procedure to solve for the IOP of the involved camera(s), EOP of the imagery, and the object coordinates of the tie points. As mentioned before, establishing a traditional calibration test field is not a trivial task, and professional surveyors are required. The next section outlines an alternative approach for camera calibration using an easy-to-establish test field comprised of a group of straight lines as well as some tie points.

Camera Calibration Using Straight Lines

Including straight lines in the bundle adjustment procedure would require addressing two main issues. First, what is the most convenient model for representing straight lines in the object and image space? Second, how to establish the perspective relationship between image and object space lines? In this research, two points are used to represent the object space straight-line (such as points A and B in Figure 1). These points are monoscopically measured in one or two images within which this line appears (such as points a' and b' in Figure 1). The relationship between these points and the corresponding object space points is modeled by the collinearity equations. It is important to note that the object coordinates of points A and B are unknowns and will be derived from the adjustment procedure. In the image space, the lines will be defined by a sequence of intermediate points along the line (such as point d in Figure 1). Similar to the end points, the intermediate points are monoscopically measured (i.e., there is no need to identify conjugate points in overlapping images). This representation is useful since it allows for continuous modeling of distortions along the linear feature. The perspective relationship between image and object space lines is incorporated in a mathematical constraint as in Equation 4:

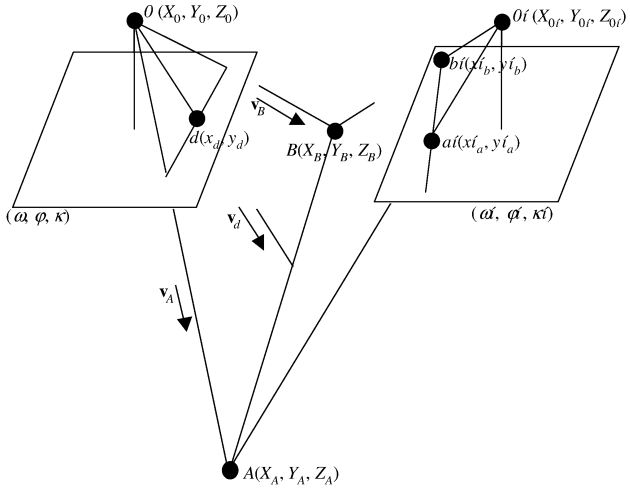

Figure 1. Mathematical model for including straight lines in images captured by frame camera.

$$(\mathbf{v}_A \times \mathbf{v}_B)\circ\mathbf{v}_d = \left(\begin{bmatrix} X_A - X_0 \\ Y_A - Y_0 \\ Z_A - Z_0 \end{bmatrix} \times \begin{bmatrix} X_B - X_0 \\ Y_B - Y_0 \\ Z_B - Z_0 \end{bmatrix}\right)\circ \left(R(\omega,\phi,\kappa)\begin{bmatrix} x_d - x_p - \Delta x \\ y_d - y_p - \Delta y \\ -c \end{bmatrix}\right) = 0 \quad (4)$$

where:

- $\mathbf{v}_A$, $\mathbf{v}_B$ are the vectors connecting the perspective center of the image under consideration and the end points A and B along the object space line,
- $\mathbf{v}_d$ is the vector connecting the perspective center of the image to an intermediate point along the image line,
- (X_A, Y_A, Z_A) are the object coordinates of point A along the object space line,
- (X_B, Y_B, Z_B) are the object coordinates of point B along the object space line,
- (X_0, Y_0, Z_0) are the object coordinates of the image exposure station,
- $R(\omega, \varphi, \kappa)$ is the rotation matrix involving the three orientation angles of the image,
- (x_d, y_d) are the image coordinates of an intermediate point along the image line,
- (x_p, y_p) are the image coordinates of the principal point,
- c is the camera principal distance, and
- $(\Delta x, \Delta y)$ are the cumulative effects of the distortion parameters as described in the previous section.

The underlying principle of this constraint is that vectors (v_A, v_B, and v_d) are coplanar (see Figure 1). Equation 4 incorporates the IOP of the camera (which includes the distortion parameters), the exterior orientation parameters, the image coordinates of the intermediate point, and the object coordinates of the points defining the object space line. The constraint in Equation 4 can be written for each intermediate point along the line in the imagery. One should note that this constraint would not introduce any new parameters. The total number of constraints is equal to the number of measured intermediate points along the image line.

The straight-line constraint in Equation 4 mainly contributes towards the estimation of the lens distortions and other deformations, which cause deviations from straightness in the image space. For determining the principal distance and the principal point coordinates of the implemented camera, distances between some targets (e.g., circled targets in Figure 2) are measured and used as additional constraints in the bundle adjustment procedure (i.e., there is no need to precisely measure their 3D coordinates). It should be noted that the same approach can be extended to include higher-order primitives (for example, conic sections). In addition, it is applicable for line cameras as well. The only difference in the line camera case is that perturbations in the motion of the platform during the scene capture, as well as the above mentioned distortion sources will cause deviations from straightness in the imagery. Habib et al., 2001, reported obtained results from implementing the proposed calibration procedure in imagery captured by line cameras.

Utilizing linear features for digital camera calibration is attractive since they can be easily extracted from the calibration imagery. The extraction and measurement of the end and intermediate points along the linear features in the imagery can proceed according to the following strategy:

1. Imagery is resampled to reduce their size. This step is needed just to speed up the extraction process.
2. An edge detection operator is applied. For example, Canny edge detection can be implemented to identify the linear features (Canny, 1986). Since we are mainly aiming at extracting straight lines with small deviations, only smooth changes in orientation are allowed in the extracted features.
3. Straight lines are identified using Hough transform (Hough, 1962). For that purpose, a parameter domain is introduced and the edge pixels, which were extracted in the previous step, are used to populate the parameter space. Peaks in the parameter space correspond to edge pixels along image space linear features. One should note that we are only looking for lines with small deviations from straightness due to the distortions. Therefore, clusters, rather than well-defined peaks, are sought for in the parameter space. The size of the cluster depends on the expected deviation from straightness in imagery of object space straight lines.
4. After identifying the straight lines in the image space, connectivity among the involved pixels is established and the extreme (end) points along each line are automatically identified. After this step, one proceeds by using the original image at full resolution.
5. Extracted end points in the previous step are then used for defining a search space for the intermediate points along the

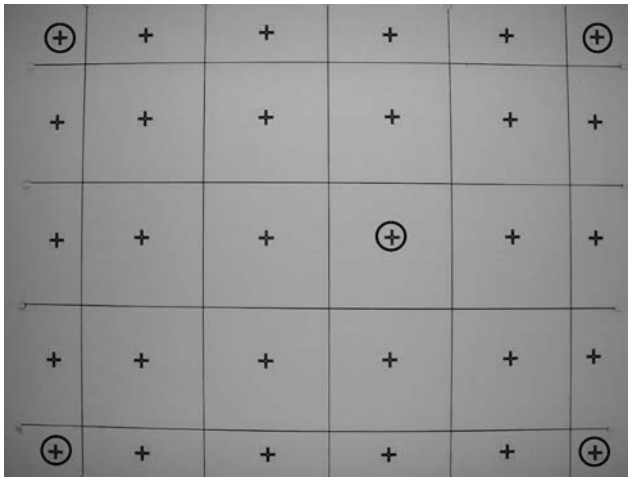

Figure 2. Test field for line-based and point-based calibration. Circled targets are used as tie points and their in-between distances are used in the line-based calibration.

lines. Profiles perpendicular to the line connecting the end points are inspected to determine the location of the intermediate points with sub-pixel accuracy by means of weighted average. Straight lines in the test field are established by using dark ropes on a bright background. Therefore, the location of the minimum gray value along the profile will be searched for. By repeating this step, one can extract numerous points along each line (Figure 3).

Having introduced a calibration procedure that requires an easy to establish test field, one should focus on the stability analysis of digital cameras. The following section discusses possible alternatives for checking camera stability by inspecting the IOP of the same camera that have been derived from two different calibration sessions.

Stability Analysis

Analog metric cameras proved to possess strong structural relationship between the elements of the lens system and the focal plane. Practical experience with these cameras showed that they maintain the stability of their IOP, although some discrepancies might be observed between in-situ and lab-derived IOP due to different imaging conditions. Shortis *et al.*, 2001 reported some analysis of digital camera stability by using the ratio of the mean precision of target coordinates to the largest dimension of the target array. However, to the best of the authors' knowledge, there has not been a comprehensive study to quantify and introduce meaningful meaures for the stability of the IOP of digital cameras for photogrammetric applications. This void in the literature can be attributed to the absence of standards for quantitative analysis of camera stability. In this section, we will present several methodologies for comparing two sets of IOP of the same camera that have been derived from two calibration sessions. The objective of the presented methodologies is to decide whether the two IOP sets are equivalent or not. It should be noted that these methodologies are general enough that they are applicable for stability analysis of analog and/or digital cameras.

The first and most obvious strategy for comparing the IOP is based on statistical testing. The following section briefly outlines the use of statistical testing to check camera stability as well as expected drawbacks. Then, the discussion proceeds by introducing a new methodology for stability analysis based on the degree of similarity between the reconstructed bundles using two sets of IOP.

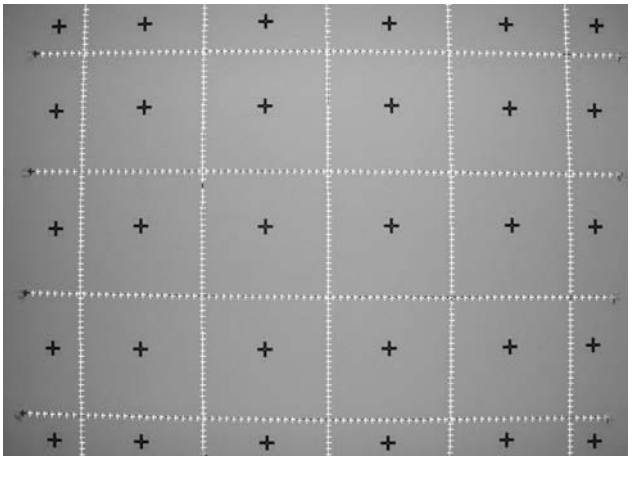

Figure 3. Automatically extracted linear features.

Statistical Testing

Let us assume that the same camera has been calibrated twice, the estimated IOP from the two sessions are IOP_I and IOP_{II}, and the corresponding variance-covariance matrices are Σ_I and Σ_{II}, respectively. For statistical testing, a probabilistic distribution, which describes the statistical properties of each respective IOP, has to be assumed. For lack of a better knowledge, IOP_I and IOP_{II} can be assumed to follow a normal distribution with a mean of the true IOP of the implemented camera, and variance-covariance matrices of Σ_I and Σ_{II}, respectively. Such distribution can be mathematically described as follows:

$$IOP_I \sim \left(IOP,\ \Sigma_I\right) \ \& \ IOP_{II} \sim \left(IOP, \Sigma_{II}\right)$$

For stability analysis, one can introduce and check the validity of a null hypothesis (H_o), which assumes the equivalence of the two IOP sets. Accepting such hypothesis verifies the stability of the tested camera. On the other hand, rejecting the null hypothesis indicates an implicit acceptance of the alternative hypothesis (H_a). In other words, we are testing the validity of either one of the following two hypotheses:

$$H_o: IOP_I = IOP_{II} \qquad \text{versus} \qquad H_a: IOP_1 \neq IOP_{II}$$

Assuming that the true IOP of the implemented camera did not change between the two calibration sessions, one can rewrite the null hypothesis as follows:

$$H_o: e = IOP_I - IOP_{II} \sim (0, \Sigma_I + \Sigma_{II})$$

One should note that the modified null hypothesis assumes that the two estimates of the IOP are statistically independent (i.e., IOP_I and IOP_{II} are not correlated). For such a hypothesis, a test statistic (T) can be computed as follows:

$$T = e^T \left(\Sigma_I + \Sigma_{II}\right)^{-1} e$$

The test statistic (T) follows a χ^2 distribution with degrees of freedom that is equal to the rank of the matrix $(\Sigma_I + \Sigma_{II})$, Koch, 1999. Assuming certain level of significance (i.e., probability of rejecting true null hypothesis), one can make a decision whether the estimated IOP are significantly different from each other or not.

One can argue that camera stability analysis using statistical testing has the following problems:

- It assumes normal distribution for the estimated IOP without any biases.
- It assumes the availability of the variance-covariance matrices associated with multiple estimates of the IOP. This might not be always the case.
- It does not consider possible correlation between IOP and EOP.
- Regardless of whether the estimates of the IOP are significantly different from each other or not, one cannot quantify the differences between the respective bundles in terms of the quality of the reconstructed object space.

These drawbacks mandate the development of stability analysis techniques, which quantitatively describe the degree of similarity between the reconstructed bundles using the available IOP.

Similarity of Reconstructed Bundles

The ultimate objective of camera calibration is reconstructing a bundle of light rays (as defined by the perspective center and image points along the focal plane) that is as similar as possible to the incident bundle on the camera at the moment of exposure. Therefore, stability analysis using IOP derived from different calibration sessions should be based on a quantitative evaluation of the degree of similarity between the reconstructed bundles.

The IOP describe the location of the perspective center relative to the focal/image plane as well as various distortions, along the image plane, taking place during the image formation process. Therefore, connecting the perspective center with distortion-free points along the focal plane defines a bundle of light rays. Using two IOP sets, one can define two bundles of light rays (Figure 4a and 4b). The question concerned with camera stability is whether these bundles are similar or not. The degree of similarity between these bundles can be evaluated by computing the spatial angle (angular offset) between conjugate light rays, while assuming that the two bundles share the same perspective center and the image coordinate systems associated with the two bundles are parallel to each other, Figure 4c. Accordingly, the derivation of a quantitative measure for the degree of similarity between the two bundles can proceed as follows:

- Define a synthetic regular grid in the image plane.
- Use the available IOP from different calibration sessions to remove various distortions at the defined grid vertices.
- Use the principal distance, principal point coordinates, and distortion-free coordinates of the grid vertices to define two bundles of light rays (Figures 4a and 4b).
- Compute the spatial angle between conjugate light rays within the defined bundles in the previous step.
- Derive statistical measures describing the magnitude and variation among the estimated spatial angles.

As mentioned before, the above methodology for comparing the reconstructed bundles assumes the coincidence of the optical axes defined by the two IOP sets (i.e., the image coordinate systems associated with the two bundles are parallel to each other (Figure 4c)). However, for stability analysis, we are mainly interested in whether the reconstructed bundles coincide with each other or not, regardless of the orientation of the respective image coordinate systems. Therefore, one should check if there is a unique set of three rotation angles (e.g., ω, ϕ, κ) that can be applied to the first bundle to produce the second one while maintaining the same perspective center (Figure 4d). In order to determine these rotation angles, let's start by defining the vectors connecting the perspective center and distortion-free grid vertices using both sets of IOP. As shown in Figure 4d, (x_I, y_I, $-c_I$) and (x_{II}, y_{II}, $-c_{II}$) are the three-dimensional vectors connecting the perspective center and two conjugate distortion-free coordinates of the same grid vertex according to IOP_I and IOP_{II}, respectively. To make the two vectors coincide with each other, the first vector has to be rotated using three rotation angles (ω, ϕ, κ) until it is aligned along the second vector. This coincidence of the two vectors after applying the rotation angles can be mathematically expressed as follows:

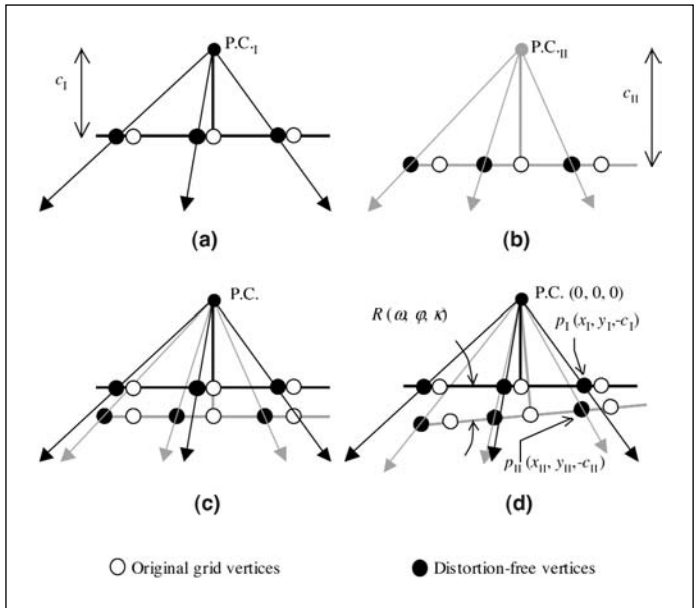

Figure 4. Illustration of distortion-free bundles using (a) IOP_I and (b) IOP_{II}, (c) the two bundles sharing the same perspective center while keeping the image coordinate systems parallel, and (d) after allowing spatial rotation.

$$\begin{bmatrix} x_{II} \\ y_{II} \\ -c_{II} \end{bmatrix} = \lambda\, R(\omega,\phi,\kappa) \begin{bmatrix} x_I \\ y_I \\ -c_I \end{bmatrix} \tag{5}$$

To eliminate the scale factor (λ), one can divide the first two rows in Equation 5 by the third one after multiplication with the transpose of the rotation matrix:

$$\begin{aligned} x_I &= -c_I \frac{r_{11}\, x_{II} + r_{21}\, y_{II} - r_{31}\, c_{II}}{r_{13}\, x_{II} + r_{23}\, y_{II} - r_{33}\, c_{II}} \\ y_I &= -c_I \frac{r_{12}\, x_{II} + r_{22}\, y_{II} - r_{32}\, c_{II}}{r_{13}\, x_{II} + r_{23}\, y_{II} - r_{33}\, c_{II}}. \end{aligned} \tag{6}$$

Equation 6 represents the necessary constraints for making the two bundles defined by IOP_I and IOP_{II} coincide with each other. Defining a regular grid of $n \times n$ points along the image plane would yield ($2n^2$) constraints. Using least squares adjustment, one can derive an estimate of the rotation angles (ω, ϕ, κ). The variance component (σ_0^2), the variance of an observation of unit weight, resulting from the adjustment procedure represents the quality of the coincidence between the two bundles after applying the estimated rotation angles. However, further analysis of the variance component would yield a more meaningful measure of the degree of similarity between the two bundles.

Assuming that (x_I, y_I) in Equation 6 are the observed values, the corresponding residuals represent the deviation between the coordinates (x_I, y_I) and the computed coordinates by back projecting the rotated vector (x_{II}, y_{II}, $-c_{II}$) to the image plane defined by the first set of IOP. In other words, the residuals represent the spatial offset between the two bundles, after applying the rotation angles, along the image plane defined by the first IOP set. Therefore, assigning a unit weight to all the constraints resulting from various grid vertices yields a *variance component that represents the variance of the spatial offset between the two bundles along the image plane*. A relative comparison between the computed variance component and the expected variance of image coordinate measurements would reveal whether the two bundles are significantly different from each other or not. In addition to the variance component, one can compute the angular offset between second bundle defined by IOP_{II} and the rotated bundle defined by IOP_I (i.e., after applying the estimated rotation angles).

So far, we have developed meaningful and quantitative measures of the degree of similarity between two bundles of light rays, defined by two sets of IOP, sharing the same origin (perspective center). However, it is expected that the IOP and EOP might be correlated. Therefore, it is important to develop additional measures for comparing the bundles in terms of their fit at a given object space.

Object Space Comparison of the Bundles

To allow for possible correlation between the IOP and EOP, one should permit spatial and rotational offsets between the two bundles while observing their fit at a given object space

(i.e., the two bundles might not share the same perspective center), Figure 5. The proposed methodology for evaluating the degree of similarity between the two bundles in terms of their fit at a given object space can proceed as follows:

- Define a regular grid in the image plane.
- Using two estimates of the IOP, derive distortion-free coordinates of the grid vertices.
- Define a bundle of light rays using the perspective center together with the distortion-free grid vertices according to the first set of IOP.
- Intersect the bundle with an *arbitrary object space* to produce a set of object points.
- Use the object points and the corresponding distortion-free grid vertices, according to the second set of IOP, in a Single Photo Resection (SPR) procedure to estimate the position and the attitude of the second bundle that fits the object space as defined by the given set of object points.
- The variance component resulting from the SPR procedure represents a quantitative measure of the spatial offset between the distortion-free grid vertices, defined by the second set of IOP, and the computed coordinates from back projecting the object points.
- A relative comparison between the computed variance component and the expected variance of the image coordinate measurements will reveal whether the two bundles would fit at the object space or not.

Now, we would like to discuss the relevance of the choice of the object space for producing the ground control points for the SPR procedure. A relatively flat terrain would most probably yield a better fit between the two bundles at the object space, even if the two IOP sets were significantly different from each other. This should be expected since such a scenario would result in high correlations between EOP and IOP. In other words, EOP would change to absorb the differences between the two IOP sets. On the other hand, a rugged terrain gives a more reliable measure for the degree of similarity between the two bundles. Such a terrain would allow for the de-correlation between IOP and EOP. Therefore, one can choose the type of terrain in such a way that it is similar to the expected object space to be photographed by the calibrated camera.

In summary, two methodologies have been introduced to check camera stability by comparing two sets of IOP that have been derived from two calibration sessions. The first measure is defined by determining the quality of the coincidence between conjugate light rays within two reconstructed bundles sharing the same perspective center. One should note the two bundles are allowed to rotate relative to each other until the best coincidence is achieved. The other approach, allows for possible spatial and rotational offsets between the two bundles while observing their quality of fit at a given object space. The second approach is expected to yield a more relaxed stability measure, especially when assuming a relatively flat terrain. Due to correlations between the EOP and IOP, the two bundles will change their position and attitude in space to ensure a good fit at the object space.

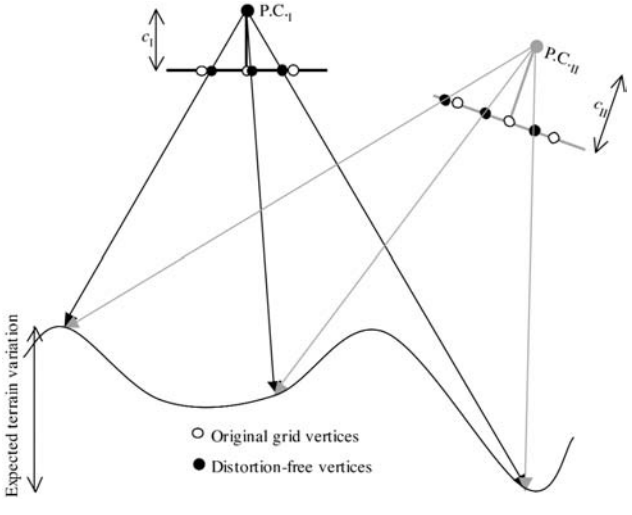

Figure 5. Comparison between the distortion-free bundles in terms of their fit at the object space.

Experimental Results

To prove the feasibility of the suggested line-based calibration procedure, we conducted an experiment to compare the estimated IOP using a traditional point-based calibration test field with these derived from a test field comprised of a group of straight lines, Figure 2. For this experiment, we used a SONY DSC-F707 digital camera, with a maximum resolution of 2560 × 1920 pixels (pixel size = 4 μm). A test field composed of nine straight lines (black ropes on a white background) is established as shown in Figure 2. The straightness of the linear features has been realized by using light material for the ropes and applying adequate tension. The test field is approximately 3 m × 3 m. Distances between five targets have been measured with an accuracy of ±2.0 mm (circled targets in Figure 2). To compare the suggested line-based and traditional point-based calibration procedures, the test field has been augmented with signalized targets. A total of 30 targets in the same test field are precisely surveyed using a total station (±0.5 mm). Twelve converging images, at six different locations roughly three meters away from the test field, are captured. Estimated IOP using these targets in a point-based calibration procedure are shown in Table 1. The developed automatic procedure for measuring the end and intermediate point coordinates along the lines in the involved imagery is implemented. The image coordinate measurements of the tie points, associated with the distance measurements, as well as measured points along the lines are incorporated in a line-based calibration procedure to derive an estimate of the IOP, Table 1. By comparing the estimated IOP from the point-based and the suggested line-based calibration procedures, one concludes that both calibration procedures resulted in equivalent numerical values for the IOP of the implemented camera. Moreover, comparing the standard deviations of the estimated parameters, one can see that the line-based approach is superior to the one that is point-based. This is attributed to the increased redundancy from considering numerous intermediate points along the linear features as well as a better recovery of the distortion parameters by the line-based approach.

To check the stability of the estimated IOP, the same camera is calibrated after ten months of regular use, as well as ground shipping between two locations thousands of miles away from each other (IOP_{II}, IOP_{III} – Table 2). The only differ-

TABLE 1. POINT AND LINE-BASED CALIBRATION RESULTS OF THE SONY CAMERA

	Point Based	Line Based
x_p (mm)	−0.1247 (±0.0040)	−0.1224 (±0.0016)
y_p (mm)	−0.0707 (±0.0042)	−0.0642 (±0.0015)
c (mm)	11.6041 (±0.0118)	11.6034 (±0.0048)
K_1 (mm^{-2})	−1.118769e-03	−1.174221e-03

TABLE 2. CALIBRATION RESULTS FROM MULTIPLE LINE-BASED CALIBRATION SESSIONS OF THE SONY CAMERA

	IOP_I	IOP_{II} (10 months later)	IOP_{III} (10 months later)
x_p (mm)	−0.1224	−0.0924	−0.1651
y_p (mm)	−0.0642	−0.0538	−0.0610
c (mm)	11.6034	11.6262	11.6543
K_1 (mm^{-2})	−1.174221e-003	−1.234290 e-003	−1.670030 e-003
K_2 (mm^{-4})	0.0	0.0	1.479427 e-005
P_1 (mm^{-1})	0.0	0.0	−1.628873 e-004

ence between IOP_{II} and IOP_{III} is that the former considered only one coefficient for the radial lens distortions while the latter considered two coefficients for the radial lens distortion as well as another coefficient for the de-centering lens distortion. For stability analysis, one should decide on whether IOP_I, IOP_{II}, and IOP_{III} are significantly different from each other or not.

The degree of similarity between IOP_{II} and IOP_{III}, is first checked using statistical testing by introducing the null hypothesis (H_o: $IOP_{II} = IOP_{III}$). Using the estimated parameters as well as the associated variance-covariance matrices, the test statistic (T) is found to be 8077, which follows a χ^2-distribution with six degrees of freedom. Assuming a level of significance of 0.005, the test statistic critical value for accepting the null hypothesis is 18.55, which leads to the rejection of the null hypothesis (i.e., IOP_{II} and IOP_{III} are significantly different from each other). Afterwards, the degree of similarity between the reconstructed bundles is used to compare IOP_{II} and IOP_{III}. The mean angular offset between the two bundles, while assuming parallel image coordinate systems, is computed, Table 3. Then, we estimated the rotation angles that are needed to make the two bundles coincide with each other as well as possible. After applying the estimated rotation angles, the mean angular offset between the bundles is significantly smaller and the square root of the estimated variance component from the adjustment procedure is not significantly larger than the expected image coordinate measurement accuracy (roughly half a pixel), Table 3. Therefore, it is concluded that IOP_{II} and IOP_{III} are almost identical. Comparing the results from statistical testing and the suggested approach for checking the stability analysis, one concludes that statistical testing would lead to a pessimistic evaluation of the stability of the implemented camera even if the reconstructed bundles from the two IOP sets are almost identical. Therefore, the degree of similarity between the reconstructed bundles offers a more realistic measure of camera stability. Consequently, further experiments for stability analysis are only based on checking the degree of similarity between the reconstructed bundles.

To check the stability of the camera over long time periods, we considered the degree of similarity between the reconstructed bundles using IOP_I and IOP_{II}. The mean angular offset between conjugate light rays, while assuming parallel image coordinate systems, is shown in Table 3. However, after rotating the two bundles relative to each other to ensure better coincidence resulted in a reduced mean angular offset. The square root of the estimated variance component from the adjustment procedure turned out to be approximately half of a pixel, which lies within the acceptable range of expected image coordinate measurement accuracy. Therefore, it is concluded that IOP_I and IOP_{II} are almost identical. This signifies the stability of the implemented camera over ten-month period.

Another set of stability analysis experiments has been conducted using a CANON EOS-1D digital camera, with a maximum resolution of 2464 × 1648 pixels (pixel size = 11.5 μm). Table 4 shows calibration results for this camera from two different calibration sessions that have been provided to the authors without any further details about the implemented calibration procedure. The angular offset between conjugate light rays within the reconstructed bundles from these parameters, while assuming parallel image coordinate systems, has a mean value of 264″ ± 7409″. The constraints, described by Equation 6, are then used to estimate the rotation angles needed to make the two bundles coincide with each other as close as possible. The square root of the estimated variance component from the adjustment procedure is 0.721154 mm, which is almost equivalent to an offset of sixty-three pixels in the image plane. Such an offset is much larger than the expected range of image coordinate measurement accuracy. Therefore, it is concluded that the two bundles are different from each other.

As mentioned earlier, the two bundles can be compared by checking their fit at a given object space while allowing spatial and rotational offsets between their origins. For such a comparison, one can derive a set of object coordinates by projecting distortion-free grid vertices using IOP_I into an arbitrary object space. These coordinates are then used in a SPR procedure using distortion-free image coordinates of the corresponding grid vertices using IOP_{II}. In this experiment, we used two extreme object space configurations. The first object space represents a hilly terrain that lies at 1000 m from the perspective center with height variation of ±800 m. The second object space represents a flat terrain with a distance of 1000 m from the perspective center. The estimated SPR parameters together with the variance component for the hilly and flat terrain can be seen in Table 5. For the hilly terrain, the estimated variance component from the SPR $(0.722544\ mm)^2$ is close to that estimated by comparing the two bundles sharing the same origin, $(0.721154\ mm)^2$. The similarity of the estimated variance components should be expected since a hilly terrain would decouple any correlation between the IOP and EOP, thus yielding a reliable evaluation of the degree of similarity between the reconstructed bundles (note the small shift components between the origins of the two bundles – Table 5). Using flat terrain, the square root of the estimated variance component from the SPR procedure turned out to be approximately 0.04 pixels, which indicates a good fit between the two bundles at flat object space. One should be careful that this is a very optimistic and might be a deceiving conclusion. In such a case, a flat terrain would lead to high correlation between the IOP and EOP. Therefore, although the two bundles are significantly

TABLE 3. ANGULAR OFFSET COMPARISON OF THE DISTORTION-FREE BUNDLES OF THE SONY CAMERA

	Comparing IOP_{II} & IOP_{III}		Comparing IOP_I & IOP_{II}	
	Before Rotation	After Rotation	Before Rotation	After Rotation
Mean angular offset	1292″ ± 43″	−2″ ± 54″ $\sigma_0^2 = (0.0025mm)^2$ $= (0.6\ pixels)^2$	543″ ± 50″	−12″ ± 65″ $\sigma_0^2 = (0.0029mm)^2$ $= (0.7\ pixels)^2$

TABLE 4. CALIBRATION RESULTS FROM MULTIPLE CALIBRATION SESSIONS OF THE CANON CAMERA

	IOP_I	IOP_{II}
x_p (mm)	0.2576	0.0194
y_p (mm)	0.0059	0.0022
c (mm)	25.2420	28.4691
K_1 (mm^{-2})	−8.170912 e-005	−8.037934 e-005

TABLE 5. SPR RESULTS FOR THE CANON CAMERA

	SPR Results Using Hilly Terrain	SPR Results Using Flat Terrain
X_0 (m)	0.0159 (±0.0033)	7.5137 (±0.0013)
Y_0 (m)	−0.0217 (±0.0041)	−0.5084 (±0.0018)
Z_0 (m)	−0.1047 (±0.0182)	−113.4797 (±0.0003)
ω''	−100.372 (±45.798)	−13.086 (±0.399)
ϕ''	−1883.465 (±44.057)	−197.938 (±0.277)
κ''	1.552 (±149.215)	0.069 (±0.077)
σ_0^2	(0.722544 mm ≈ 63 pixels)^2	(0.000420 mm ≈ 0.04 pixels)^2

different from each other, the EOP will adapt to absorb the differences between the two IOP sets to produce a good fit at the object space (note the large shift components between the origins of the two bundles: Table 5).

As far as the second camera is concerned, we could not make a decision whether the camera is not stable or that the IOP have been determined using unfavorable imaging configuration. However, if this camera to be used to capture imagery over relatively flat terrain, one should expect a similar quality of the reconstructed object space using either set of IOP. This equivalence is only possible if no constraints are introduced regarding the position and/or the attitude of the exposure station, since the EOP should be allowed to change their values to ensure a good fit at the object space. In other words, for indirect orientation applications using this camera over relatively flat terrain, one can utilize either set of IOP, while ensuring the same quality of the reconstructed object space.

Conclusions and Recommendations for Future Work

The presented research in this paper outlined an efficient approach for camera calibration using an easy-to-establish test field comprised of a group of straight lines and few signalized targets. The distance between the targets are measured and introduced as additional constraints in the bundle adjustment to allow for the estimation of the principal distance and the coordinates of the principal point. On the other hand, deviations from straightness in the image space linear features contribute towards to the estimation of lens distortions. A framework for automatic extraction of the linear features has been also presented. Experimental results with real data showed that the IOP derived from the suggested line-based calibration procedure is better than those estimated using traditional calibration utilizing distinct control points.

In addition, several alternatives for checking camera stability have been introduced. It has been established that statistical testing would not yield reliable measures of the stability of the IOP of the implemented camera due to the stringent assumptions of that approach. A more realistic and meaningful measure of camera stability can be derived by quantitatively evaluating the degree of similarity between reconstructed bundles using different IOP sets. The degree of similarity can be established by computing the mean angular offset between conjugate light rays after allowing some rotational offset between the respective bundles to ensure that they coincide with each other as well as possible. Stability analysis of two digital cameras revealed that the IOP of the first camera remained unchanged over a ten-month period of regular and repetitive use.

A more relaxed stability measure can be derived by checking the quality of fit between the reconstructed bundles at a given object space. In this case, the defined bundle using one set of IOP is projected into an arbitrary object space to produce a set of object points. These points, together with the corresponding bundle defined by the other set of IOP, are used in a SPR procedure to evaluate the quality of fit between the two bundles at the given object space. It has been established that a rugged terrain would produce a realistic estimate of the degree of similarity between the two bundles since it would decouple possible correlation between the EOP and IOP. On the other hand, a flat terrain would yield an optimistic measure of the quality of fit at the object space since it leads to high correlation between the IOP and EOP. In other words, the EOP would change to absorb the differences between the two IOP sets to produce a good fit at the object space.

It should be noted that the introduced calibration technique and stability measures are general enough that they can be applied to digital as well as analog cameras intended for mapping applications. The combination of the line-based calibration procedure and the introduced stability measures would allow amateur users of digital cameras to evaluate their IOP and stability. Current research will continue to focus on short and long-term stability of off-the-shelf digital cameras under different handling and operational modes. In addition, the effect of the quality of the available IOP on the reconstructed object space from direct and indirect geo-referencing procedures will be investigated for various types of terrain. Based on the results from stability analysis by checking the quality of fit between the reconstructed bundles at the object space, one expects that for direct orientation, special attention has to be paid towards a reliable calibration of the involved camera. On the other hand, for indirect orientation, the quality of the IOP is not as critical, especially if we are dealing with relatively flat terrain. Current research aims at verifying this prediction.

References

Bräuer-Burchardt, C., and K. Voss, 2001. A new algorithm to correct fish-eye and strong wide-angle-lens-distortion from single images, *Proceedings of the 2001 International Conference on Image Processing*, October 07–10, Thessaloniki, Greece, Volume 1, pp. 225–228.

Brown, D., 1966. Decentric distortion of lenses, *Photogrammetric Engineering & Remote Sensing*, 32(3):444–462.

Brown, D., 1971. Close range camera calibration, *Photogrammetric Engineering & Remote Sensing*, 37(8):855–866.

Canny, J., 1986. A computational approach to edge detection, *IEEE Transactions on Pattern Analysis and Machine Intelligence*, 8(6):679–698.

Chen, S., and W. Tsai, 1990. A systematic approach to analytic determination of camera parameters by line features, *Pattern Recognition*, 23(8):859–877.

Fraser, C., 1997. Digital camera self-calibration, *ISPRS Journal of Photogrammetry and Remote Sensing*, 52(4):149–159.

Fryer, J., 1996. Camera calibration, *Close Range Photogrammetry and Machine Vision*, (K.B. Atkinson, editor), Whittles Publishing, Caithness, Scotland, pp. 156–180.

Guoqing, Z., U. Ethrog, F. Wenhao, and Y. Baozong, 1998. CCD camera calibration based on natural landmarks, *Pattern Recognition*, 31(11):1715–1724.

Koch, K., 1999. *Parameter Estimation and Hypothesis Testing in Linear Models*, Second Edition, Springer-Verlag, Berlin, Heidelberg, 333p.

Kraus, K., 1997. Choice of Additional Parameters, *Photogrammetry, Volume 2 – Advanced Methods and Applications*, Dümmler/ Bonn, pp. 133–136.

Habib, A., Y. Lee, and M. Morgan, 2001. Bundle Adjustment with Self-Calibration of Line Cameras using Straight Lines, *Joint Workshop of ISPRS WG I/2, I/5 and IV/7: High Resolution Mapping from Space 2001*, University of Hanover, 19–21 September, Unpaginated CD Rom.

Habib, A., M. Morgan, and Y. Lee, 2002a. Bundle Adjustment with Self-Calibration using Straight Lines, *The Photogrammetric Record*, 17(100):635–650.

Habib, A., S. Shin, and M. Morgan, 2002b. New Approach for Calibrating Off-The-Shelf Digital Cameras, *ISPRS Symposium of PCV'02 Photogrammetric Computer Vision*, Graz, Austria, 09–13 September, Unpaginated CD Rom.

Heuvel, F., 1999. Estimation of interior orientation parameters from constraints on line measurements in a single image, *Proceedings of International Archives of Photogrammetry and Remote Sensing*, Thessaloniki, Greece, 07–09 July, 32(5W11):81–88.

Hough, 1962. Methods and Means for Recognizing Complex Patterns, *U.S. Patent 3,069,654*.

Prescott, B., and G. McLean, 1997. Line-Based Correction of Radial Lens Distortion, *Graphical Models and Image Processing*, 59(1):39–47.

Shortis, M., C. Ogleby, S. Robson, E. Karalis, and H. Beyer, 2001. Calibration Modelling and Stability Testing for the Kodak DC200 Series Digital Still Camera, *Proceedings of SPIE on Videometrics and Optical Methods for 3D Shape Measurements*, San Jose, California, 22–23 January, Volume 4309, pp. 148–153.

(Received 21 November 2003; accepted 10 March 2004; revised 15 August 2004)